

# Counteracting Enantiospecific Behavior of Tailor-Made Additives During Chiral Symmetry Breaking: Growth Inhibition *versus* Solid-Solution Formation

Iaroslav Baglai,<sup>\*,[a, b]</sup> Sjoerd W. van Dongen,<sup>[a]</sup> Michel Leeman,<sup>[c]</sup> Richard M. Kellogg,<sup>[c]</sup> Bernard Kaptein,<sup>[d]</sup> and Willem L. Noorduin<sup>\*,[a, c]</sup>

*Dedicated to Prof. Meir Lahav and Prof. Leslie Leiserowitz in honor of the 2021 Wolf prize in Chemistry.*

**Abstract:** All biological systems are composed of molecules of a single chirality. Although many different scenarios can lead to chiral symmetry breaking, the transmission of the absolute configuration of one compound to another one remains challenging. We here demonstrate that during crystallization-induced chiral symmetry breaking by Viedma ripening, a cascade of different and counteracting processes

can occur: solid-solution formation and dissolution inhibition favor symmetry breaking towards the same absolute configuration, while enantioselective growth inhibition favors symmetry breaking towards the opposite absolute configuration. These insights offer a new playground for controlling symmetry breaking processes that are of fundamental and practical importance.

**Keywords:** crystallization · chiral symmetry breaking · Viedma ripening · deracemization · solid solution

Homochirality is a sign of life.<sup>[1–3]</sup> At the molecular level, all living organisms are composed of chiral building blocks – exclusively (L)-amino acids and (D)-sugars. Complete chiral symmetry breaking and the propagation of homochirality play a crucial role in the discussion on the origin of life scenarios. Tremendous efforts aimed to provide a scientific explanation of this phenomenon resulted into an intriguing Frank model,<sup>[4]</sup> followed by discoveries of the Soai reaction<sup>[5]</sup> and Viedma ripening (*i.e.* attrition-enhanced deracemization).<sup>[6,7]</sup> Although the Soai reaction enables complete symmetry breaking, it remains a unique example and its underlying principles are not readily extendable to prebiotic systems. Viedma ripening has been proven as a remarkably powerful and versatile approach for chiral amplification with a variety of compounds; in particular with derivatives and precursors of amino acids.<sup>[8–16]</sup> Viedma ripening can be applied to any racemizable conglomerate – a chiral compound that crystallizes as enantiomorphous crystals while undergoing racemization in the liquid phase. Upon Viedma ripening, a continuous dissolution-crystallization process coupled to racemization enables complete conversion of racemic solid phase of a slurry into a single enantiomer of choice.<sup>[7]</sup> To direct a process towards the desired enantiomer, a well-controlled initial symmetry breaking is required. Creating a tiny enantiomeric excess (*ee*) in the desired enantiomer in the solid phase has been shown as the most practical way of controlling the outcome.<sup>[12,13,17]</sup> Circularly polarized light<sup>[18,19]</sup> and even the order of events<sup>[20,21]</sup> have also been demonstrated as effective symmetry breaking controllers in Viedma ripening processes.

Lahav and Leiserowitz provided fundamental frameworks for understanding the influence of enantiomerically pure

additives on chiral symmetry breaking during crystallization.<sup>[22,23]</sup> The additives interact enantioselectively with enantiomorphs of a racemic conglomerate. Additives can absorb stereospecifically on the surface of the enantiomorph of the same absolute configuration and thereby inhibit its further growth. As a result, the solid phase becomes enriched in the enantiomer of the opposite absolute configuration to the additive (Figure 1A). This kinetically driven enantiospecific growth inhibition and its consequences on symmetry breaking are well-described by the “rule of reversal”.<sup>[22,23]</sup> Lahav and Leiserowitz have also developed an approach to steer crystallization towards a desired handedness by designing

[a] Dr. I. Baglai, Mr. S. W. van Dongen, Prof. Dr. W. L. Noorduin  
AMOLF, Science Park 104, 1098 XG Amsterdam, The Netherlands  
E-mail: noorduin@amolf.nl

[b] Dr. I. Baglai  
Ardena Amsterdam BV, Meibergdreef 31 1105 AZ Amsterdam, The Netherlands  
E-mail: iaroslav.baglai@gmail.com

[c] Dr. M. Leeman, Prof. Dr. R. M. Kellogg  
Symeres, Kadijk 3, 9747 AT Groningen, The Netherlands

[d] Dr. B. Kaptein  
InnoSyn BV, Urmonderbaan 22, 6167 RD Geleen, The Netherlands

[e] Prof. Dr. W. L. Noorduin  
Van 't Hoff Institute for Molecular Sciences, University of Amsterdam, 1090 GD Amsterdam, The Netherlands

© 2021 The Authors. Israel Journal of Chemistry published by Wiley-VCH GmbH. This is an open access article under the terms of the Creative Commons Attribution License, which permits use, distribution and reproduction in any medium, provided the original work is properly cited.

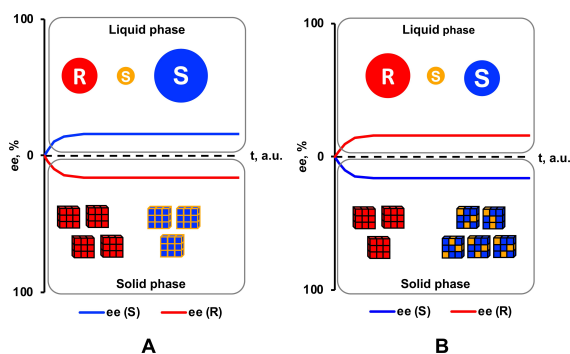


**Figure 1.** Schematic illustration of initial chiral symmetry breaking driven by enantiomerically pure additive upon crystallization. A) Enantiospecific growth inhibition favors crystallization of the enantiomer of the opposite configuration. B) Enantiospecific solid solution formation favors crystallization of the enantiomer of the same absolute configuration. Distribution of the *ee* over time between the liquid and solid phases shown with blue (S-configuration) and red (R-configuration) lines.

“tailor-made additives” for deliberate stereospecific inhibition of crystal growth.<sup>[22,24]</sup>

On the other hand, enantiomerically pure additives are also known to form enantiospecific solid solutions with structurally and stereochemically similar compounds by incorporating into the bulk crystal lattice of enantiomorphs of the same absolute configuration.<sup>[25–29]</sup> This phase stability manipulation may result into the solid phase enantioenrichment in the configuration of the additive (Figure 1B).

Recently, we have shown that grinding of conglomerate crystals in the presence of an enantiopure additive can result in enantiospecific solid-solution formation which directs chiral symmetry breaking towards the configuration of the additive used. Amplification of this enantioid imbalance using Viedma ripening offers a mechanism for the propagation of homochirality.<sup>[30]</sup> Moreover, a detailed study of the initial symmetry breaking that occurs during grinding a slurry of racemic conglomerate in the presence of a high additive loading (20 wt%) confirmed that two antagonistic processes occur simultaneously during this stage: enantiospecific growth inhibition and enantiospecific solid solution formation (Figure 1).<sup>[30]</sup> The resulting *ee* detected in the liquid and solid phases corresponds to the difference in the relative contributions of these two processes. It has been shown that contributions of kinetically-driven enantiospecific growth inhibition are dominant initially. Nevertheless, approximately after 2 hours of grinding, the contributions of thermodynamically-controlled enantiospecific solid solution formation become larger, resulting into a switch of “signs” of chirality of the liquid and solid phases of the slurry (Figure 2).

This switch results into an enrichment of the solid phase in the enantiomer of the same absolute configuration as the additive used. As expected for a typical Viedma ripening process, initiating racemization at this point, results in the solid phase deracemization towards the configuration of the

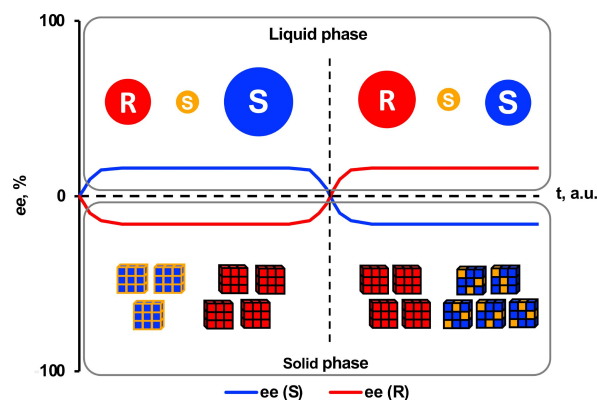
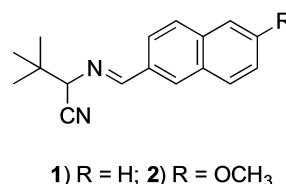


**Figure 2.** Schematic illustration pathway of chiral symmetry breaking in the presence of an enantiomerically pure additive that forms enantiospecific solid solution. Shown *ee* corresponds to the difference between the contributions of two antagonistic processes: enantiospecific growth inhibition and enantiospecific solid solution formation. Distribution of the *ee* over time between the liquid and solid phases shown with blue (S-configuration) and red (R-configuration) lines.

majority population, thus towards the absolute configuration of the additive. Remarkably, even a low additive loading (*i.e.* 5 wt%) is sufficient to direct deracemization towards the configuration of the additive.<sup>[30]</sup> Nevertheless, it remains unclear whether the initial symmetry breaking follows the pathway identical to that observed with a high additive loading (Figure 2), or if the contributions of the solid solution formation take over the contributions of the enantiospecific growth inhibition.

In the current study, we examine the evolution of the additive-driven chiral symmetry breaking at a low additive loading. To this aim we ground a slurry of (*RS*)-**1** in the presence of an enantiomerically pure additive (*S*)-**2** that forms enantiospecific solid solution with conglomerate **1** (Scheme 1).

Specifically, a slurry of (*RS*)-**1** was equilibrated at 21 °C for 1 hour by sonication in the presence of glass beads to accelerate continuous growth/dissolution. Then, the enantiomerically pure additive (*S*)-**2** (5 wt%, below the solubility limit) was added to initiate the additive-driven chiral symmetry breaking. The resulting slurry was further sonicated at 21 °C, while the compositions of the liquid and solid phases were monitored by HPLC analyses of samples taken over time.



**Scheme 1.** Chemical structures of compound **1** and the additive **2**.

Chiral symmetry breaking starts as soon as the additive is introduced into the slurry. The initial symmetry breaking occurs accordingly to the “rule of reversal”. The present (*S*)-2 additive acts as an enantiospecific growth inhibitor of the (*S*)-1 enantiomorph. The (*R*)-1 enantiomorph grows faster, resulting into an enantioenrichment of the solid phase with a chirality that is opposite to the additive configuration. Contrary to the high additive loading (20 wt%) experiment, where the contributions of enantiospecific growth inhibition are being overtaken by those of the solid solution formation within approximately 2 hours, the switch in the “signs” of chirality (Figure 2) was not observed even after 19 hours of sonication. At a low additive loading, the contributions of enantiospecific growth inhibition remains more significant, maintaining the solid phase enriched in *R* – the opposite configuration to the additive (Figure 3). Thus, by initiating a Viedma ripening process at this point, one would expect deracemization of the solid phase towards the majority population, towards the *R* enantiomer.<sup>[31]</sup> Remarkably, the analysis of the first sample of the slurry taken after the addition of a racemization catalyst – 1,8-diazabicyclo[5.4.0]undec-7-ene (DBU) - showed that the solid phase switched the “sign” of chirality, it became enriched in the (*S*)-1 enantiomer. Further grinding of the slurry led to complete deracemization of the solid phase to the *S* configuration (Figure 3). Note that the presence of DBU in the liquid phase ensures a nearly instantaneous racemization of compounds 1 and 2. Indeed, no *ee* is detected in the liquid phase after addition of DBU.

Our observations during the experiment indicate three key stages of the complete symmetry breaking: 1) initial symmetry breaking; 2) switch of the solid phase “sign” of chirality; 3) chiral amplification of the *ee* created during the initial symmetry breaking in stage 1 (Figure 3). Whereas the observed initial symmetry breaking can be explained by effects of kinetically-driven growth inhibition following the rule of reversal, and the *ee* amplification stage by a typical

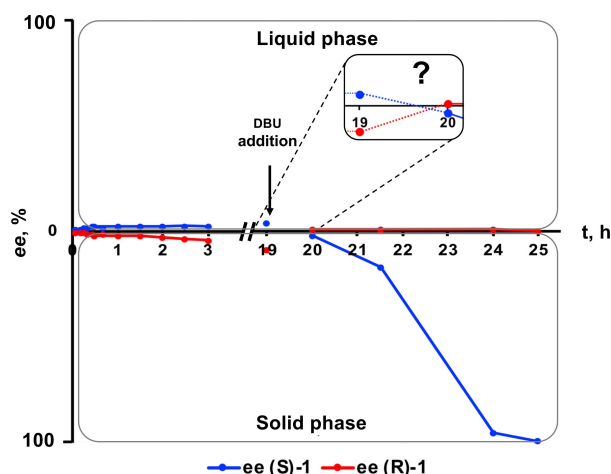


**Figure 3.** Enantiomeric excess evolution of 1 during a 5 wt% (*S*)-2 additive-driven complete symmetry breaking.

Viedma ripening process, the switch in the solid phase “sign” of chirality and its drivers remain intriguing.

The presence of an internal standard in the slurry enabled monitoring of the absolute concentrations of the compounds present in the liquid phase (Figure 4). These data reveal that a simple act of adding DBU results into a cascade of counter-acting processes: it not only initiates racemization of compounds 1 and 2 in the liquid phase, but also significantly increases solubilities of (*R*)-1 and (*S*)-1 (Figure 4). These processes have consequences. The additive (*S*)-2 present in the liquid phase racemizes providing (*R*)-2 that can form an enantiospecific solid solution with (*R*)-1, favoring enrichment of the solid phase in the *R* configuration. And, obviously, both enantiomers of the additive 2 can act as enantiospecific growth inhibitors of both enantiomorphs (*R*)-1 and (*S*)-1. Additionally, the observed changes in the absolute concentrations (Figure 4) suggest an extra dissolution of the solid phase. As initially shown by Lahav and Leiserowitz, enantiomerically pure additives may act not only as enantiospecific growth inhibitors upon crystallization, but also as enantiospecific dissolution inhibitors upon dissolution.<sup>[22]</sup> Thus, relative contributions of the listed phenomena are likely to cause the observed switch in the “sign” of the solid phase chirality triggered by the DBU addition.

The broken symmetry of life’s building blocks has inspired fascinating questions ever since Pasteur’s initial discovery. Although many different scenarios can lead to chiral symmetry breaking,<sup>[32]</sup> transmission of the absolute configuration of one compound to the other is still mysterious. From this perspective, enantiospecific solid solution formation in combination with Viedma ripening offers a promising scenario as it enables complete chiral symmetry breaking towards the configuration of the additive used, thus offering a powerful mechanism for the propagation of homochirality.

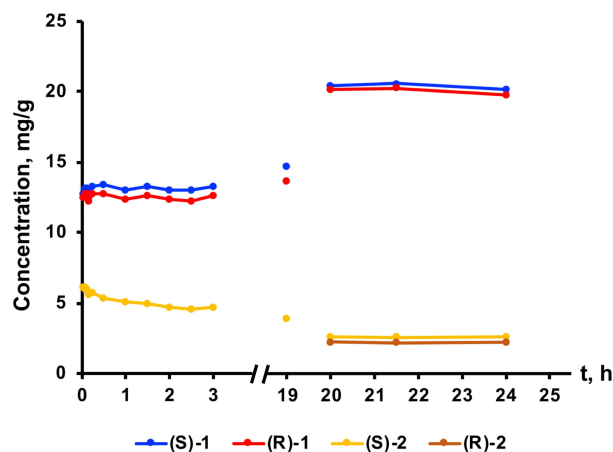


**Figure 4.** Absolute concentrations of the compounds in the liquid phase. Note, the addition of DBU also initiates racemization of the additive (*S*)-2, resulting into the formation of (*R*)-2 that forms solid solution with (*R*)-1.

As we show here, during chiral symmetry breaking, a cascade of different and counteracting processes can occur simultaneously, leading to very complex behavior even though the system has a small number of interacting components. Specifically, we identify the following phenomena that act and counteract with each other during the symmetry breaking and first stages of chiral amplification: solid-solution formation and dissolution inhibition favor symmetry breaking towards the absolute configuration of the additive, while enantiospecific growth inhibition favors symmetry breaking towards the opposite absolute configuration.

These results highlight the importance of subtle effects that can lead to completely different outcomes and in particular the role of kinetics in these processes. A logical next step will be to disentangle these counteracting processes. Hence, the fundamental lessons of Lahav and Leiserowitz on chiral molecular interactions developed over the past decades will remain most relevant for the advances in the journey of understanding the broken symmetry of life.

## Experimental Section

### Additive-Driven Symmetry Breaking Followed by Deracemization

A screw cap 20 mL vial was charged with 2 mm glass beads (10 g), (*RS*)-**1** (1.0 g) and stock solution of anisole (0.2 wt% internal standard) in MeOH (10 mL). The vial was placed in an ultrasonic bath equipped with a thermostat, and sonicated for 1 hour at 21 °C. Subsequently, the enantiomerically pure additive (*S*)-**2** was added to the slurry. The sonication of the resulting mixture was continued at 21 °C. After 19 hours of sonication, 1,8-diazabicyclo[5.4.0]undec-7-ene (DBU) (0.3 mL) was added to the slurry to initiate racemization. Subsequently, the slurry was sonicated for 6 hours to achieve complete deracemization of the solid phase. The resulting suspension was replaced into a P4 filter, using a Pasteur's pipet to separate the suspension and glass beads, and filtered. The isolated solid was rinsed with MeOH (2 × 0.5 mL) and dried to afford a white solid (270 mg; ee > 99%; (*S*)-**2** incorporation 1.3%, by area). Please note that the given isolated yield is not corrected neither on compound **1** that stays in the liquid phase (appr. 400 mg, see Figure 4) nor on the sampling (the total volume of the slurry sampled out is appr. 3 mL (30% of the starting slurry). Samples of the slurry (appr. 0.15 mL each) were taken over time. The liquid and solid phases were separated by filtration through a syringe filter (0.2 µm) and analyzed by HPLC on a chiral column.

## Acknowledgements

This work was supported by AMOLF funds for Topsector-related research and IXAnext Physics2Market grant. SWVD

and WLN acknowledge OCENW.KLEIN.155, which is financed by the Dutch Research Council (NWO).

## References

- [1] J. L. Bada, *Nature* **1995**, 374, 594–595.
- [2] J. L. Bada, *Chem. Soc. Rev.* **2013**, 42, 2186–2196.
- [3] W. H. P. Thiemann, U. Meierhenrich, *Origins Life Evol. Biospheres* **2001**, 31, 199–210.
- [4] F. C. Frank, *Biochim. Biophys. Acta* **1953**, 11, 459–463.
- [5] K. Soai, T. Shibata, H. Morloka, K. Choji, *Nature* **1995**, 378, 767–768.
- [6] C. Viedma, *Phys. Rev. Lett.* **2005**, 94, 065504.
- [7] W. L. Noorduin, W. J. P. van Enkevort, H. Meekes, B. Kaptein, R. M. Kellogg, J. C. Tully, J. M. McBride, E. Vlieg, *Angew. Chem. Int. Ed.* **2010**, 49, 8435–8438; *Angew. Chem.* **2010**, 122, 8613–8616.
- [8] W. L. Noorduin, T. Izumi, A. Millemaggi, M. Leeman, H. Meekes, W. J. P. Van Enkevort, R. M. Kellogg, B. Kaptein, E. Vlieg, D. G. Blackmond, *J. Am. Chem. Soc.* **2008**, 130, 1158–1159.
- [9] C. Viedma, J. E. Ortiz, T. De Torres, T. Izumi, D. G. Blackmond, *J. Am. Chem. Soc.* **2008**, 130, 15274–15275.
- [10] L. Spix, A. Alfring, H. Meekes, W. J. P. Van Enkevort, E. Vlieg, *Cryst. Growth Des.* **2014**, 14, 1744–1748.
- [11] L. Spix, H. Meekes, R. H. Blaauw, W. J. P. Van Enkevort, E. Vlieg, *Cryst. Growth Des.* **2012**, 12, 5796–5799.
- [12] M. van der Meijden, M. Leeman, E. Gelsens, W. L. Noorduin, H. Meekes, W. J. P. van Enkevort, B. Kaptein, E. Vlieg, R. M. Kellogg, *Org. Process Res. Dev.* **2009**, 13, 1195–1198.
- [13] P. Wilmink, C. Rougeot, K. Wurst, M. Sanselme, M. Van Der Meijden, W. Saletta, G. Coquerel, R. M. Kellogg, *Org. Process Res. Dev.* **2015**, 19, 302–308.
- [14] L. B. Spix, *Deracemizing Racemic Compounds*, Radboud Universiteit Nijmegen, **2015**.
- [15] B. Kaptein, W. L. Noorduin, H. Meekes, W. J. P. Van Enkevort, R. M. Kellogg, E. Vlieg, *Angew. Chem. Int. Ed.* **2008**, 47, 7226–7229; *Angew. Chem.* **2008**, 120, 7336–7339.
- [16] I. Baglai, M. Leeman, K. Wurst, B. Kaptein, R. M. Kellogg, W. L. Noorduin, *Chem. Commun.* **2018**, 54, 10832–10834.
- [17] I. Baglai, M. Leeman, R. M. Kellogg, W. L. Noorduin, *Org. Biomol. Chem.* **2019**, 17, 35–38.
- [18] W. L. Noorduin, A. A. C. Bode, M. van Der Meijden, H. Meekes, A. F. van Etteger, W. J. P. van Enkevort, P. C. M. Christianen, B. Kaptein, R. M. Kellogg, T. Rasing, et al., *Nat. Chem.* **2009**, 1, 729–732.
- [19] M. Sakamoto, N. Uemura, R. Saito, H. Shimobayashi, Y. Yoshida, T. Mino, T. Omatsu, *Angew. Chem. Int. Ed.* **2021**, 60, 12819–12823.
- [20] W. L. Noorduin, H. Meekes, W. J. P. Van Enkevort, B. Kaptein, R. M. Kellogg, E. Vlieg, *Angew. Chem. Int. Ed.* **2010**, 49, 2539–2541; *Angew. Chem.* **2010**, 122, 2593–2595.
- [21] I. Baglai, M. Leeman, B. Kaptein, R. M. Kellogg, W. L. Noorduin, *Chem. Commun.* **2019**, 55, 6910–6913.
- [22] L. Addadi, S. Weinstein, E. Gati, I. Weissbuch, M. Lahav, *J. Am. Chem. Soc.* **1982**, 104, 4610–4617.
- [23] L. Addadi, Z. Berkovitch Yellin, N. Domb, E. Gati, M. Lahav, L. Leiserowitz, *Nature* **1982**, 296, 21–26.
- [24] I. Weissbuch, D. Zbaida, L. Addadi, L. Leiserowitz, M. Lahav, *J. Am. Chem. Soc.* **1987**, 109, 1869–1871.
- [25] C. Garcia, A. Collet, *Tetrahedron: Asymmetry* **1992**, 3, 361–364.

- [26] M. Vaida, L. J. W. Shimon, Y. Weisinger-Lewin, F. Frolow, M. Lahav, L. Leiserowitz, R. K. McMullan, *Science* **1988**, *241*, 1475–1479.
- [27] J. M. McBride, *Angew. Chem. Int. Ed.* **1989**, *28*, 377–379; *Angew. Chem.* **1989**, *101*, 391–393.
- [28] A. Collet, L. Ziminski, C. Garcia, F. Vigné-Maeder, in *Supramol. Stereochem.*, Springer Netherlands, Dordrecht, **1995**, pp. 91–110.
- [29] M. Leeman, J. M. De Gooier, K. Boer, K. Zwaagstra, B. Kaptein, R. M. Kellogg, *Tetrahedron: Asymmetry* **2010**, *21*, 1191–1193.
- [30] I. Baglai, M. Leeman, K. Wurst, R. M. Kellogg, W. L. Noorduin, *Angew. Chem. Int. Ed.* **2020**, *59*, 20885–20889; *Angew. Chem.* **2020**, *132*, 21071–21075.
- [31] T. P. T. Nguyen, P. S. M. Cheung, L. Werber, J. Gagnon, R. Sivakumar, C. Lennox, A. Sossin, Y. Mastai, L. A. Cuccia, *Chem. Commun.* **2016**, *52*, 12626–12629.
- [32] D. G. Blackmond, M. Klussmann, *Chem. Commun.* **2007**, 3990–3996.

Manuscript received: July 31, 2021  
Version of record online: September 13, 2021